Article:

Alsaif, A, Bernal, SA, Guadagnini, M et al. (1 more author) (2018) Durability of steel fibre reinforced rubberised concrete exposed to chlorides. Construction and Building Materials, 188. pp. 130-142. ISSN 0950-0618

https://doi.org/10.1016/j.conbuildmat.2018.08.122

Durability of Steel Fibre Reinforced Rubberised Concrete Exposed to Chlorides

Abdulaziz Alsaif[a*], **Susan A. Bernal**[b], **Maurizio Guadagnini**[a]
Kypros Pilakoutas[a]

[a]Department of Civil and Structural Engineering, The University of Sheffield, Sir Frederick Mappin Building, Mappin Street, Sheffield, S1 3JD, UK.

[b]Department of Materials Science and Engineering, The University of Sheffield, Sir Robert Hadfield Building, Mappin Street, Sheffield, S1 3JD, UK

[*] Corresponding author: email: asaalsaif1@sheffield.ac.uk; Tel: +44 (0) 114 222 5729, Fax: +44 (0) 114 2225700

Abstract

This study assesses the durability and transport properties of steel fibre reinforced rubberised concrete (SFRRuC) which is proposed as an alternative construction material for flexible pavements. Waste tyre rubber is incorporated in concrete as fine and coarse aggregate replacement and blends of manufactured steel fibres and recycled tyre steel fibres are used as internal reinforcement. The fresh, mechanical and permeability properties of plain concrete are compared with those of SFRRuC mixes having different substitutions of rubber aggregates (0, 30 and 60% by volume). The chloride corrosion effects due to exposure to a simulated accelerated marine environment (intermittent wet-dry cycles in 3% NaCl solution) is also evaluated. The results show that, although permeability (volume of permeable voids, sorptivity and chloride penetration and diffusion) increases with rubber content, this increase is minor and permeability properties are generally within the range of highly durable concrete mixes. No visual signs of deterioration or cracking (except superficial rust) were observed on the surface of the concrete specimens subjected to 150 or 300 days of accelerated chloride corrosion exposure and a slight increase in the mechanical properties is observed. The study confirms SFRRuC as a promising candidate for flexible pavements with good durability and transport properties.

Keywords: *Rubberised concrete; Steel fibre reinforced concrete; Hybrid reinforcement; Flexible concrete pavement.*

1 Introduction

Several factors are considered when designing road pavements including traffic loading, sub-grade status, environmental conditions, as well as cost and availability of construction materials. Two different systems of pavements are conventionally used in roads construction: flexible asphalt or rigid concrete. The design of flexible pavement is based on the load distributing characteristics of the component layers, whilst the design of rigid concrete pavements is based on flexural strength or slab action. Flexible asphalt pavements can better accommodate local deformations arising from loads and soil movements, but lack the durability of rigid concrete pavements that are by nature much stiffer [1]. It is therefore desirable to develop a pavement system with comparable flexibility to asphalt pavement, and ability to withstand higher stresses as well as environmental attack during its service life. One attractive alternative proposed by the authors is concrete pavements that include high amounts of recycled rubber particles (chips and/or crumbs), as a partial replacement of natural aggregates, and recycled steel fibre reinforcement. These composite concretes, referred to as steel fibre reinforced rubberised concretes (SFRRuC), can be designed to have low stiffness values similar to asphalt and flexural strengths similar to conventional concrete [1].

Over the past two decades, research interest in the potential use of waste tyre rubber (WTR) as partial replacement of natural aggregates in the production of concretes (rubberised concretes – RuC) has steadily grown [2-6]. RuC present reduced workability and increased air content, compared to conventional concretes, as a result of the rough surface texture of the rubber particles [4, 7-9]. Though RuC can develop relatively high ductility and strain capacity, as well as increased toughness and energy dissipation compared to conventional concrete [8-10], this is generally accompanied by a reduction in strength and stiffness [11, 12]. As a result, RuC have been mainly used in low-strength non-structural applications (e.g. concrete pedestrian blocks or lightweight fills). Different strategies to improve the mechanical performance of RuC have been investigated in recent years, including the addition of supplementary cementitious materials to the binder mix to reduce the porosity and aid early age strength development. Increases in the compressive strength of RuC of up to 42% has been achieved [2] when using 10 wt.% silica fume and fly ash as partial replacement of Portland cement in the concrete mixes.

The addition of fibres to RuC can enhance the mechanical performance of these composite concretes. Xie et al. [13] reported that the addition of manufactured steel fibres (MSF) in RuC, mitigated the reduction in compressive strength while increasing residual flexural strength. Similar outcomes were reported in other studies by the authors [1, 2] where SFRRuC presented better compressive and flexural behaviour as well as a higher energy absorption than plain RuC. Although the fresh and mechanical properties of RuC and SFRRuC have been studied by several researchers, there is still a dearth of data, especially when both fine and coarse natural aggregates are replaced with rubber particles in the large volumes (exceeding 20% by volume of total aggregates) necessary to achieve flexible concrete pavements.

Few studies examined the durability and transport properties of RuC, with notable discrepancies being reported on the effect of rubber particles on long-term performance. Water permeability and water absorption by immersion generally increase with rubber content [14-16]. This has been attributed to the additional water required in RuC mixes to maintain workability, and the high void volumes between rubber particles and cement paste due to the hydrophobicity of rubber. Conversely, several researchers have observed a decrease in water absorption of RuC (up to 12.5% rubber for fine aggregates) using the method of immersion and related this behaviour to the impervious nature of rubber particles. Benazzouk et al. [17] reports that the addition of rubber crumbs of up to 40% volume in cement pastes reduced sorptivity, hydraulic diffusivity and air permeability. Similar observations are reported by Segre & Joekes [18] who also attributed this behaviour to the hydrophobic nature of rubber. The transport properties of these composite concretes are strongly dependent on the distinctive features of the starting concrete matrix, whose performance can significantly vary as a function of mix design, age and curing conditions, among other factors, which explains the variability in results obtained from different investigations.

In a recent study, the authors [1] investigated the mechanical properties of SFRRuC mixes with rubber particles used as partial replacement of both fine and coarse aggregates (0%, 20%, 40% or 60% replacement by volume), and different types of steel fibres (MSF and/or recycled tyre steel fibres- RTSF) added in volumes of up to 40 kg/ m^3. It was concluded that all of the examined SFRRuC mixes are promising candidate materials for use in structural concrete applications with increased toughness and flexibility requirements, such as road pavements and slabs on grade, and meet the flexural strength characteristics described in pavement design standard EN 13877-1[54]. Concrete pavement slabs, however, are susceptible to several deteriorative processes that can be caused by the transport of aggressive substances in concrete, such as corrosion due to attack by chlorides or carbonation. The rate of transport of aggressive agents is highly related to the water movement contained in a porous volume, whether in liquid or vapour form, and to air permeability [17]. Aggressive substances such as chlorides can also penetrate into concrete due to diffusion and capillary action.

The chloride permeability in RuC remains largely unknown and studies examining this [19, 20] reveal increased chloride permeability with rubber content, which can be significantly reduced with the addition of fly ash and/or silicate fume. This is consistent with the reduced water absorption and permeability achieved in concretes with these additions. To the best of the authors' knowledge, only limited information is available on the transport and durability properties of RuC with large volumes of rubber replacement [7, 21, 22], while the transport and durability properties of SFRRuC has not been studied yet. Furthermore, there is limited understanding on the mechanism governing chloride-induced corrosion of steel fibres in RuC and its potential effect on long-term performance. However, there is a good consensus that the main factors controlling durability of steel fibre reinforced concrete (SFRC), when exposed to chlorides, include: (i) exposure conditions and age, (ii) type and size of the steel fibres, (iii) quality of the concrete matrix and (iv) the presence of cracks [23]. Consequently, it is necessary to understand the transport and durability properties of SFRRuC before using it in flexible concrete pavements.

In this study, the fresh state, mechanical strength, and permeability properties of SFRC, and SFRRuC are investigated and compared. The fresh properties assessed include workability, air content and fresh density. The mechanical performance is examined in terms of compressive strength and flexural behaviour including flexural strength, elastic modulus and residual flexural strength. The permeability properties examined are volume of permeable voids, gas permeability, sorptivity and chloride penetrability (chloride ion penetration depth and diffusion). The chloride corrosion effects due to exposure to a simulated accelerated marine environment (intermittent wet-dry cycles in 3% NaCl solution) are also evaluated.

2 Experimental Programme

2.1 Materials and mix designs

2.1.1 Materials

A high strength Portland lime cement CEM II-52.5 N, containing around 10–15% limestone in compliance with EN 197-1 [24], was used as primary binder to produce the assessed concretes. Pulverised fuel ash (PFA) and silica fume (SF) were used as partial replacements of the Portland cement (10 wt.% for each) in order to optimize the particle packing in the mixture, enhance concrete strength and reduce permeability. Two types of high range water reducer HRWR admixtures, plasticiser and superplasticiser, were also added to achieve the desired workability. A water/binder (Portland cements + silica fume + fly ash) ratio of 0.35 was used in all mixes.

Natural round river gravel and medium grade river washed sand were used as coarse and fine aggregates, respectively, in the manufacture of concretes. The coarse aggregates with particle sizes of 5/10 mm and 10/20 mm had specific gravity (SG) of 2.65 and water absorption (A) of 1.2%, while the fine aggregates with particles sizes of 0/5 mm had SG of 2.64 and A of 0.5%.

The rubber aggregates were recovered by the mechanical shredding of vehicular tyres. Rubber particles were sourced in the following size ranges: 0/0.5 mm, 0.5/2 mm and 2/6 mm, 5/10 mm, and 10/20 mm. A linear gradation was used to determine the portion of each particle size and a relative density of 0.8 (measured by the authors using a representative volume of rubber) was used for the rubber to determine the appropriate replacement by volume. Fig. 1 shows the particles size distribution for the used natural and rubber aggregates, obtained according to ASTM C136 [25].

A blend of two different types of steel fibres were used: 1) undulated MSF, and b) cleaned and screened recycled tyre steel fibres (RTSF). The physical and mechanical properties of both types of steel fibre are shown in Table 1.

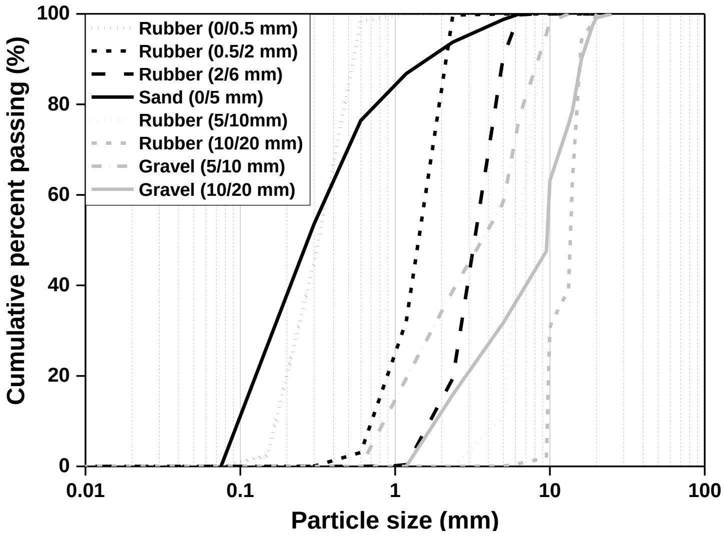

Fig. 1 Particle size distributions for natural aggregates and rubber particles

Table 1. Physical and mechanical properties of steel fibres

Fibre type	Length (mm)	Diameter (mm)	Density (g/cm3)	Tensile strength MPa
MSF	55	0.8	7.8	1100
RTSF	15-45 (> 60% by mass)	<0.3	7.8	2000

2.1.2 Concrete mix designs

An optimized concrete mix design with targeted compressive strength of 60 MPa (cylinder) at 28 days of curing, typically used in bridge piers, as developed by Raffoul et al. [9], was adopted in this study. It was confirmed by the authors in a previous study [1] that this mix design suites the replacement up to 60% of WTR without excessive degradation in fresh properties, yet maintaining a mechanical performance suitable for pavement construction.

The key parameters examined in this study were: (i) rubber content, used as partial replacement of both fine and coarse aggregates (0%, 30% and 60% replacement by volume), (ii) fibres content (0 or a blend of 20 kg/m^3 MSF + 20 kg/m^3 RTSF), (iii) curing conditions (mist room or 3% NaCl), (iv) age of testing (28, 90, 150 or 300 days).

Four different concrete mixes were cast and assessed. The mix characteristics and ID assigned to each mix are reported in Table 2 and the mix proportions for 1 m^3 are shown in Table 3. The mix ID follows the format NX, where N denotes the amount of rubber content used as partial replacement of both fine and coarse aggregates (0, 30 or 60%), while X symbolizes the presence of steel fibre reinforcement and can be either P or BF (Plain or Blend of Fibres, respectively). For instance, 30BF is the rubberised concrete mix that contains 30% of rubber particles as natural aggregate replacement and consists of blend fibres (20 kg/m^3 MSF and 20 kg/m^3 RTSF).

Table 2. Concrete mixes ID and evaluated variables

Concrete mixes ID	% Rubber replacing aggregates by volume		MSF (kg/m^3)	RTSF (kg/m^3)
	Fine	Coarse		
0P	0	0	0	0
0BF	0	0	20	20
30BF	30	30	20	20
60BF	60	60	20	20

Table 3. Mixes proportions for 1 m^3 of fresh concrete

Components	Concrete mixes			
	0P	0BF	30BF	60BF
CEM II (kg/m^3)	340	340	340	340
Silica Fume (SF) (kg/m^3)	42.5	42.5	42.5	42.5
Pulverised Fuel Ash (PFA) (kg/m^3)	42.5	42.5	42.5	42.5
Aggregates 0/5 mm (kg/m^3)	820	820	574	328
Aggregates 5/10 mm (kg/m^3)	364	364	254	146
Aggregates 10/20 mm (kg/m^3)	637	637	446	255
Water (l/m3)	150	150	150	150
Plasticiser (l/m^3)*	2.5	2.5	3.25	4.25
Superplasticiser (l/m^3)	5.1	5.1	5.1	5.1
Rubber				
0/0.5 mm (kg/m^3)	0	0	16.5	33
0.5/2 mm (kg/m^3)	0	0	24.8	49.6
2/6 mm (kg/m^3)	0	0	33	66
5/10 mm (kg/m^3)	0	0	33	66
10/20 mm (kg/m^3)	0	0	57.7	115.4
Fibres				
MSF (kg/m^3)	0	20	20	20
RTSF (kg/m^3)	0	20	20	20

*It was increased as the amount of added rubber was increased (2.5-4.75 l/m^3)

2.1.3 Mixing, casting and curing procedure

Due to the limited capacity of the pan mixer used, each mix was cast in three batches. The concrete constituents were mixed according to the sequence shown in Fig. 2.

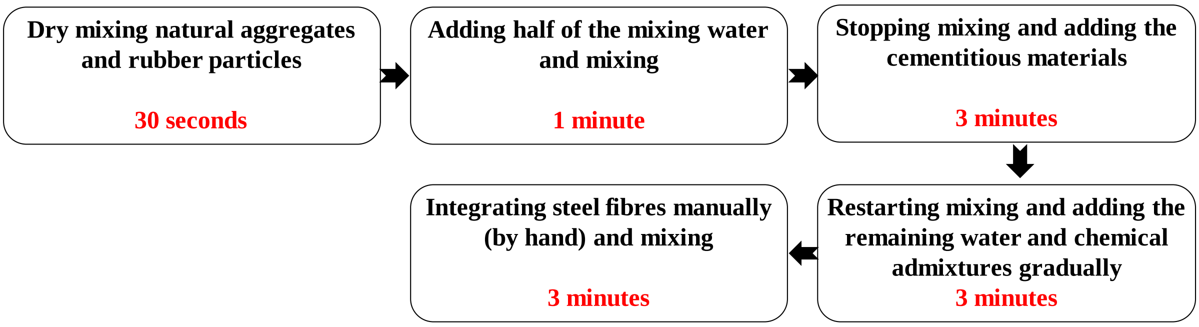

Fig. 2 Sequence of mixing

Concrete was cast in two layers (according to EN 12390-2) [26] and vibrated on a shaking table (25s per layer). The fresh concrete was covered with plastic sheets and kept under standard laboratory conditions (20 °C ± 2 and 50 ± 5 relative humidity (RH)) for 48 hrs. The specimens were then demoulded and stored in a mist room (21 °C ± 2 and 95 ± 5% RH) to cure for 28 days. Following a period of 21 days, the 150 x 300 mm and 100 x 200 mm cylinders were removed from the mist room and sliced up, parallel to the trowelled surface, into five shorter cylinders (150 x 50 mm each) and two shorter cylinders (100 x 100 mm each), respectively. All concrete slices were placed back in the mist room until the end of mist curing (28 days).

2.2 Testing methods

2.2.1 Fresh state properties

The concretes fresh properties including slump, air content and fresh density were assessed according to EN 12350-2 [27], EN 12350-7 [28], and EN 12350-6 [29], respectively.

2.2.2 Mechanical strength tests

The uniaxial compression tests were performed on concrete cubes (100 x 100 mm) according to EN 12390-3:2009 [30] at a loading rate of 0.4 MPa/s. Three specimens were tested for each of the examined concrete mixes.

The flexural behaviour of the concrete specimens was assessed by performing three-point bending tests on prisms (100 x 100 x 500 mm) with 300 mm span, similar to that suggested by RILEM [31], using an electromagnetic universal testing machine. A 5 mm-wide and 15 mm-deep notch was sawn in the concrete to force the crack formation at the mid-span and to measure the crack mouth opening displacement (CMOD) using a clip gauge (125 mm-gauge). The test was performed in CMOD control (0.005 mm/min for CMOD from 0 to 0.1 mm, 0.2 mm/min for CMOD ranging from 0.1 to 4 mm and 0.8 mm/min for CMOD from 4 mm to 8 mm). Two LVDTs mounted at the middle of a yoke (one on each side), as suggested by the JSCE [32], were used to measure the net deflection at mid-span. The flexural strength values reported in this study correspond to the average of three measurements.

2.2.3 Gas and water permeability

Cylinders of 150 x 50 mm were tested after 28 and 300 days of curing in a mist room. Prior to testing, specimens were pre-conditioned (oven dried) to remove water from the concrete pores. Rather than using the standardised preconditioning temperature of 105 ºC, which causes cracking, mainly due to the removal of interlayer and bound water present in the hydration products [33-35], a temperature of 80 ºC was initially used on the 28 day specimens in an attempt to minimise cracking. Constant mass was achieved after 7 days of drying, but SFRRuC specimens exhibited cracks of average width around 0.065 mm (Fig. 3), which can be attributed to the different coefficient of thermal expansion of the rubber aggregates. Although the values obtained from the cracked specimens are not expected to reflect the real permeability of SFRRuC, these values are still reported in the following and commented upon.

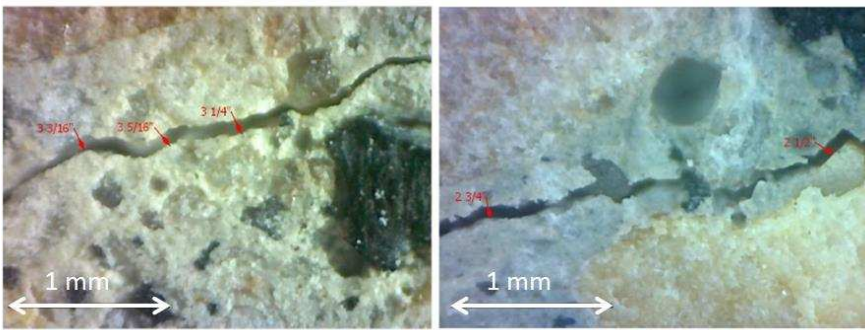

30BF **60BF**

Fig. 3 Micrographs of cracked SFRRuC specimens after pre-conditioning at 80 ºC

To minimise cracking induced during preconditioning, a reduced temperature of 40 ºC was adopted for treating the 300 day specimens. As expected, it took much longer to reach constant mass (between 30 to 40 days). Considering the extended time required to dry the concretes, it was decided not to expose the specimens to wet-dry chlorides exposure, as a direct correlation between gas and water permeability measurement and chloride penetrability would not be fair, as the concretes would have completely different ages by the time each of test was conducted.

Oxygen permeability tests followed the procedure recommended by RILEM TC 116-PCD-C [15], also called "Cembureau method", using three 150 x 50 mm cylinders per mix. Sorptivity measurements were conducted in two cylinders of similar size following the recommendation of the EN 13057 [36]. After performing the sorptivity test, the same cylinders were used to measure the volume of permeable voids (VPV) based on the procedures of ASTM C1202 [37], also called the vacuum saturation method.

2.2.4 Chloride permeability and corrosion

Chloride permeability was evaluated in two different exposure conditions: (i) fully immersing specimens in a 3% NaCl solution (placed in sealed plastic containers in the mist room until testing); and (ii) wet-dry cycles (accelerated chloride corrosion simulation), by immersion in a 3% NaCl for 4 days followed by a drying period in standard laboratory environmental conditions for 3 days. Prisms, cubes and cylinders were kept apart by at least 10 mm using a specially designed frame. All specimens were preconditioned for ion chloride penetration tests using the unidirectional non-steady state chloride diffusion-immersion method described in EN 12390-11 [38].

After preconditioning for 90, 150 and 300 days in NaCl exposure, two 100 x 100 mm cylinders per mix per condition were removed from the NaCl solution and split into two halves at mid-point according to the Nord test method NT Build 492 [39], colorimetric method. From each freshly split cylinder, the piece with the split section nearly perpendicular to the exposed surface was chosen for the penetration depth measurement, and was immediately sprayed with 0.1 N silver nitrate ($AgNO_3$) solution. Silver nitrate reacts with the chloride ion present in the hardened matrix to form white AgCl (white in colour); whereas at greater depth, silver nitrate reacts with the hydroxyl ion to form Ag_2O (dark brown), as described in formulas (1) and (2) [40].

$$Ag^{+} + Cl^{-} \rightarrow AgCl \downarrow (silver-white) \tag{1}$$

$$Ag^{+} + OH \rightarrow AgOH \rightarrow Ag_2O \downarrow (brown) \tag{2}$$

Chloride penetration depth was indicated by the boundary colour change within 10-15 minutes after spraying. The chloride penetration depth was marked at the colour change boundary and the depth was recorded as the average distance, taken from five sections (Fig. 4). The cylinder that registered the maximum average depth was selected for analysis and used to drill out binder powder from the surface and colour change boundary to determine acid-soluble chloride concentrations. Binder powders were also collected from reference specimens that were submerged in water for similar lengths of time to those immersed in the NaCl solutions in order to obtain initial chloride concentration values.

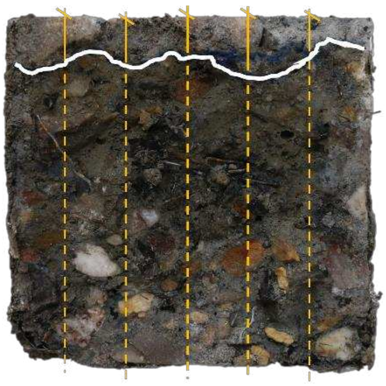

Fig. 4 Representative SFFRuC freshly split, sprayed and marked for determination of chloride penetration depth

The acid-soluble chloride concentration was measured at the 134.724 emission line using a Spectro-Ciros-Vision ICP-OES instrument which was calibrated with standards of known chloride concentrations made up in 20% nitric acid. To calculate chloride diffusion coefficients from the immersion test results, the initial chloride concentration, chloride concentrations at the surface and colour change boundary were determined and introduced to the error function solution of Fick's second law of diffusion, Eq. (3) according to the EN 12390-11 [38]:

$$C_x = C_i + (C_s - C_i)\left(1 - erf\left[\frac{x}{\sqrt{4D_{app}t}}\right]\right) \tag{3}$$

where C_x is the concentration of the chloride ion as a function of distance into the specimens x, at any time t and is taken as the maximum average chloride penetration of the depth boundary measured by silver nitrate; C_i is the initial chloride concentration; C_s is the chloride concentration at the surface; and D_{app} is the apparent diffusion coefficient.

3 Results and Discussion

3.1 Fresh state properties

The slump, air content and fresh density of the concretes studied are presented in Table 4. The addition of fibres reduced the workability of the concrete, and this effect is more notable with the inclusion of both fibres and rubber in the SFRRuC mixes. For mixes 0BF, 30BF and 60BF, the slump drops by 5%, 13% and 56%, respectively, when compared with the plain concrete, 0P. The tendency of steel fibres to agglomerate contributed to the slump reduction. The decrease in slump as a result of adding rubber particles can be explained by the higher level of inter-particle friction between rubber particles and the other concrete constituents (owing to the rough surface texture and high coefficient of friction of rubber particles) [1, 4, 7-9].

Table 4. Fresh state properties of SFRRuC evaluated. Values in parenthesis correspond to one standard deviation of three measurements

Properties	Concrete mix			
	0P	0BF	30BF	60BF
Slump (mm)	223 (14)	212 (10)	193 (15)	98 (25)
Air content (%)	1.3 (0.5)	1.4 (0.1)	3.4 (1.1)	3.2 (0.2)
Fresh density (kg/m^3)	2405 (5)	2424 (9)	2124 (6)	1859 (4)

The addition of fibres did not induce notable changes in the air content of the concrete. The substitution of natural aggregate by rubber (mixes 30BF and 60 BF), however, significantly increased the air content of the fresh concrete by more than 100%. The increased friction between fibres and rubber might cause fibres to agglomerate and trap more air. The rough and hydrophobic nature of rubber particles also tends to repel water and therefore increases the amount of entrapped air in the mix [1, 41].

The fresh density of the SFRC mix, 0BF, is slightly higher than that of the plain concrete mix, 0P, (Table 1) owing to the high specific gravity of the added fibres. The density of the fresh mix is significantly reduced when rubber particles are used to replace natural aggregates as a result of their lower density (Section 2.1.1). For the SFRRuC, 30BF and 60BF, the density decreases by 13% and 30%, respectively, compared to the plain concrete.

3.2 Effect of chloride exposure in mechanical performance

3.2.1 Visual inspection

Figs. 5 a) and b) show the appearance of specimens after 150 and 300 day exposure to accelerated chloride corrosion conditions, respectively. Prior to chloride exposure, there were no signs of rust on the concrete surface, which implies that the fibres were protected by a thin layer of cement paste. At the end of 150 days of wet-dry chloride exposure, however, the specimens showed minor signs of superficial rust (Fig. 5a) in regions where the fibres were near the concrete surface. A large amount of rust is observed on the surface of the specimens exposed for 300 days (Fig. 5b), mainly as a consequence of the corrosion of the steel frame used to hold the specimens. Nevertheless, at all periods of the accelerated chloride corrosion exposure, no sign of deterioration or cracks were observed on the concretes.

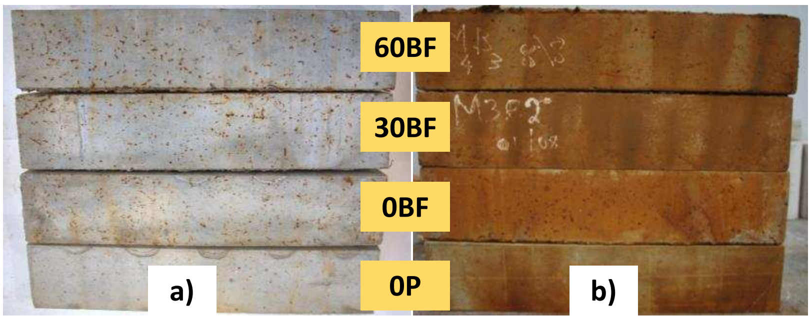

Fig. 5 SFRRuC specimens after a) 150 days, and b) 300 days of wet-dry chloride exposure

Fig. 6 shows the internal appearance of a SFRRuC splitted cube, 30BF, after 300 days of wet-dry chloride exposure. Despite the external rusty appearance (Fig. 5b), no evidence of rust is observed on the fibres embedded in these concretes. This indicates that steel reinforcement did not corrode to any significant extent under the wet-dry chloride exposure. This performance may be explained by the reduced chloride permeability of the concretes, as it will be discussed in detail in the following sections, and the discrete nature of steel fibres embedded in the matrix, generating smaller potential differences along the steel surface and reduced cathode/anode ratios compared to conventional steel rebars [23]. The uniform steel fibre surface due to cold-drawing may also contribute to the enhanced stability against chloride-induced corrosion, compared to conventional steel [42].

Fig. 6 Section through a SFRRuC specimen after 300 days of wet-dry chloride exposure

In addition, the dense and uniform fibre-matrix interfacial transition zone (ITZ), composed mainly of rich segregated lime, acts as a high alkalinity barrier and protects fibres in the bulk SFRC against chloride and oxygen ingress [23, 43]. Furthermore, even if the fibres corrode, they do not have the potential to create bursting stresses that split the surrounding concrete, as in the case of conventional rebar (see Fig. 7).

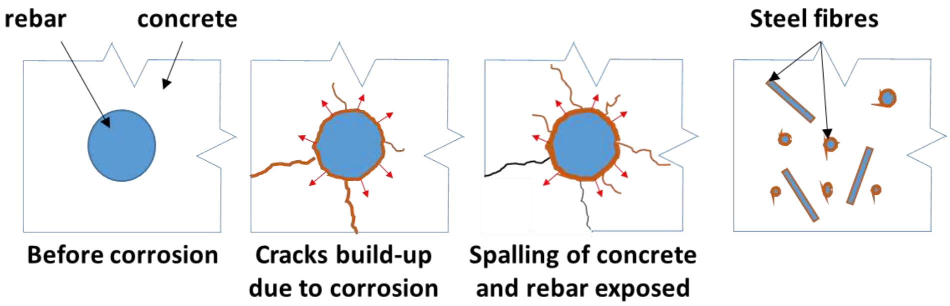

Fig. 7 Comparison between corrosion processes in conventional steel rebar and steel fibre embedded in concrete

3.3 Compressive strength

The influence of wet-dry chloride exposure on the compressive strength of SFRRuC is presented in Fig. 8. Error bars represent one standard deviation of three measurements. Comparable compressive strength values are seen for the plain concrete, 0P, and the SFRC, 0BF, before and after chloride exposure. The replacement of fine and coarse aggregates with rubber particles, however, led to a significant decrease in compressive strength. Prior to chloride exposure, reductions of up to 54% and 86% in compressive strength are seen in the SFRRuC, when 30% and 60% of fine and coarse aggregates are replaced with rubber particles, respectively. The reduction in compressive strength is mainly attributed to the lower stiffness and higher Poisson ratio of rubber compared to natural aggregates. The weak bond between cement paste and rubber particles may also contribute to the strength degradation, as discussed by the authors in [1] and Khaloo et al. in [12].

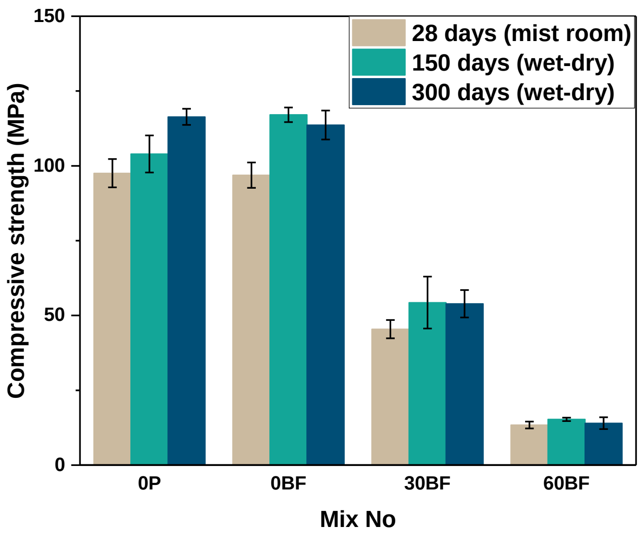

Fig. 8 Compressive strength of concretes assessed before and after 150 and 300 days of wet-dry chloride exposure

All mixes after 150 and 300 days of wet-dry chloride exposure present a slightly increased compressive strength, compared to the 28-day values measured prior to the chloride exposure. The increase in strength is attributed to the continuous hydration of the cementitious paste over the period of exposure, owing to the high amount of pozzolanic materials used for replacing Portland cement in all the concrete mixes. The addition of such supplementary cementitious materials is also expected to reduce chloride diffusivity [44], due to the combined effect of well-developed granular packing, and increase tortuosity of the pore network in the blended cementitious matrix, which improves corrosion resistance.

3.4 Flexural behaviour

The mean values of flexural strength at 28 days and after150 and 300 days of wet-dry chloride exposure are presented in Fig. 9. Error bars represent one standard deviation of three measurements. The addition of fibres to plain concrete, mix 0BF, enhances the 28-day flexural strength by 28%, with respect to the plain concrete mix, 0P. The partial replacement of natural aggregates by rubber particles reduced the flexural strength of the tested concretes, but to a lesser extent than the compressive strength (Fig. 8). The 28-day flexural strength reduction of SFRRuC mixes, 30BF and 60BF, in comparison to 0P is 12% and 44%, respectively. 0P. The contribution of steel fibres in enhancing the flexural strength was anticipated as the thin fibres, RTSF, tend to "sew" the micro-cracks that develop in the matrix during loading, while the thick fibres, MSF, tend to control the propagation of wider cracks and redistribute stresses [1, 45].

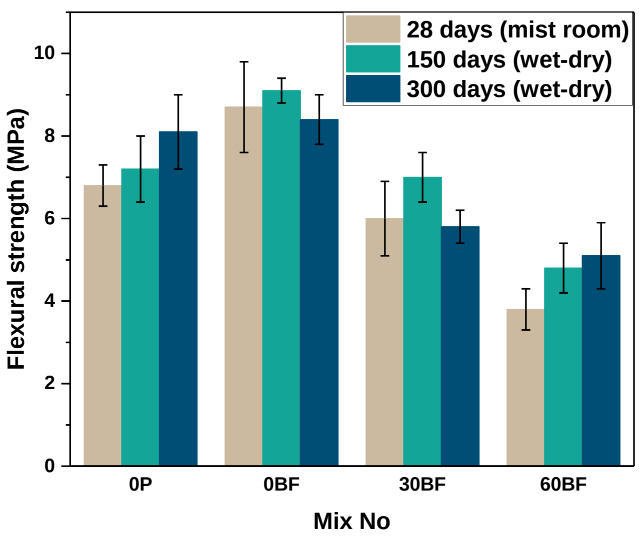

Fig. 9 Flexural strength of concretes assessed before and after 150 and 300 days of wet-dry chloride exposure

For all mixes, the flexural strength results are higher at the end of 150 days of wet-dry chloride exposure than those of 28-day mist cured specimens, as a consequence of the ongoing hydration of the cement in the concretes. Increased residual flexural tensile strength has been attributed by some authors [46] to increased roughness of the fibre surface induced by formation of corrosion products in their surface, which could increase the fibre-matrix frictional bond. However, this is unlikely to be the case here, as no internal corrosion has been observed in this work.

No clear trend can be identified in the flexural strength values of the specimens at the end of 300 days of wet-dry cycles. While 0P and 60BF mixes present higher flexural strength values, compared to those of 150 days of wet-dry cycles, the flexural strength values of 0BF and 30BF mixes are even lower than their respective strength at 28-days. This variation may be the result of the high natural variability in these specimens. It is unlikely that the flexural strength of 0BF and 30BF specimens was reduced due corrosion attack, as evidence of rust in the fibres embedded in these specimens was not observed (see Section 3.2.1).

Fig. 10 shows the average elastic modulus obtained from three prisms per mix over the three periods of testing. Error bars represent one standard deviation of three measurements. The elastic theory was used to determine the flexural elastic modulus by using the secant modulus of the load-deflection curves (from 0 to 30% of the peak load).

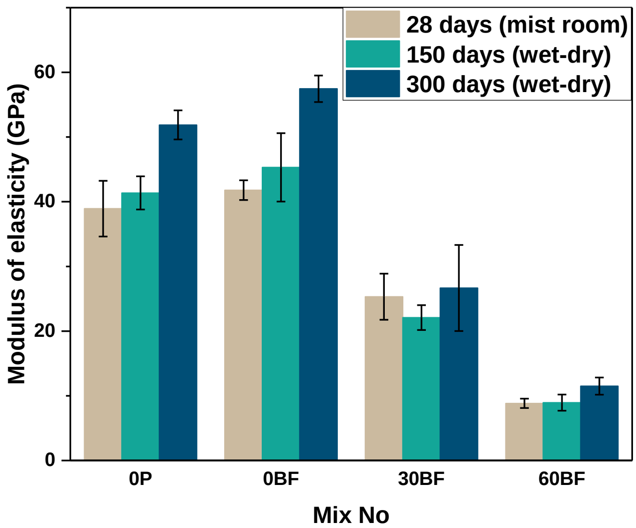

Fig. 10 Elastic modulus of all tested concrete specimens before and after 150 and 300 days of wet-dry chloride exposure

The addition of fibres induces a marginal increase in the elastic modulus of 0BF concrete compared with that of plain concrete. However, a significant reduction in the elastic modulus results from the replacement of fine and coarse aggregates with rubber particles; reductions up to 33% for 30BF and 77% for 60BF are observed, when compared to 0P. The reduction in the elastic modulus is caused mainly by the lower stiffness of the rubber particles (compared to natural aggregates) and to a lesser extent by the higher air content in these concretes, as discussed in section 3.1. Similar to the compressive and flexural strengths, a general increase in the average elastic modulus of all mixes after 150 and 300 days of wet-dry cycles was identified, compared to 28-day compressive strength.

Fig. 11 presents the average flexural stress-CMOD curves registered in all prisms over the three periods of testing. The sudden stress loss after the peak load for the plain concrete mixes indicates their brittle behaviour in tension. On the other hand, all SFRC and SFRRuC mixes show enhanced post-cracking load bearing capacity and significant energy absorption. This is a result of the fibres bridging the cracks and controlling their propagation even after the peak load, dissipating energy through pull-out and mobilising and fracturing a larger volume of concrete. It is also evident that the post-peak energy absorption behaviour of the SFRC and SFRRuC specimens is not reduced due to the accelerated wet-dry corrosion exposure, which emphasises the positive effect of the continuous hydration reaction of the cementitious matrix during testing.

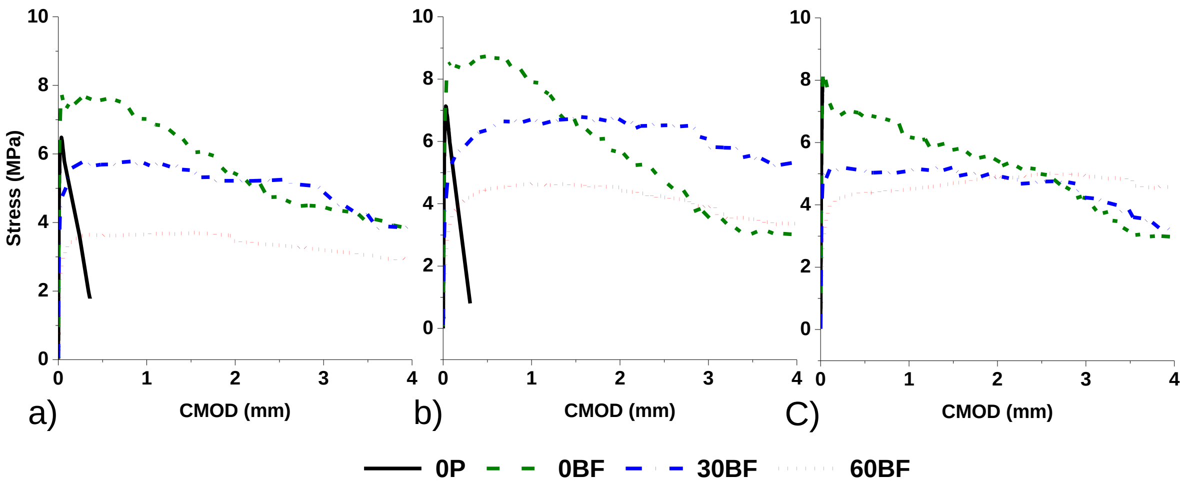

Fig. 11 Flexural stress-CMOD curves of the tested concrete specimens a) before, and after wet-dry chlorides exposure for b) 150 and c) 300 days

3.5 Transport properties

3.5.1 Evaporable moisture and volume of permeable voids

The loss of mass due to water evaporation after preconditioning the specimens at 80 ºC (28 day cured) and 40 ºC (300 day cured) was determined as the ratio between the total amount of evaporated water and the dry mass of the specimen. The mean values (average of five measurements) of evaporable moisture concentrations results, W_e, are shown in Fig. 12a, and the volume of permeable voids, VPV, are presented in Fig. 12b. Error bars correspond to one standard deviation of five measurements for W_e and two measurements for VPV. A direct relationship between the W_e and VPV is observed for all the tested concretes, independently of the preconditioning temperature and curing age, where higher values of evaporated water are obtained in more porous concretes.

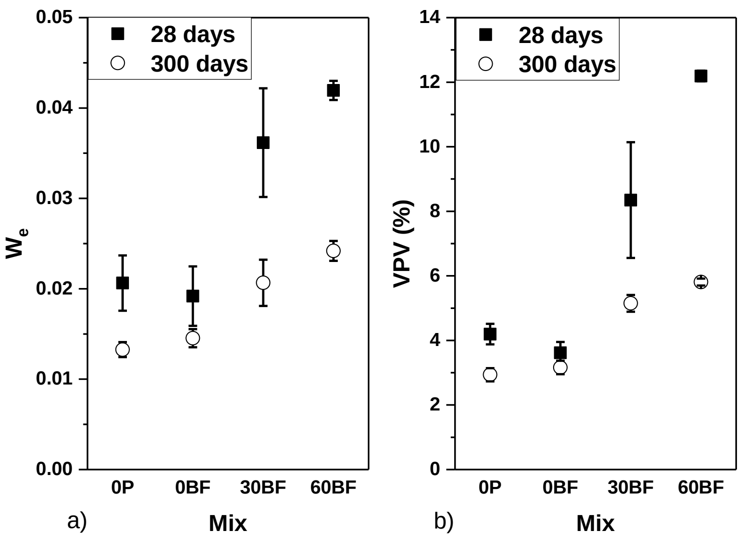

Figs. 12 a) Evaporable moisture, and b) volume of permeable voids of all tested concretes

The addition of fibres generally results in reduced shrinkage cracking and in the establishment of more tortuous and disconnected pore network [47], thus reducing VPV. For 28 days cured samples, 0BF mix exhibits, as expected, a decrease in VPV, though marginal and within the observed experimental error (average of 13%), whereas the SFRRuC mixes exhibit a large increase in VPV. This can be attributed to the rubber particles, the rough surface and hydrophobic nature of which can help trap air on their surface and make their interface more porous and highly absorptive to water [48, 49].

Minor changes in the VPV values are observed in concretes 0P and 0BF for the two curing conditions. This is unexpected as more mature concretes typically exhibit reduced permeability, but this may be the result of the already high quality of the concrete matrix evaluated in this study. In concrete composites with rubber aggregates, 30BF and 60BF, extended curing times reduce the VPV values by 24% and 93%, respectively. It should be pointed out that SFRRuC specimens exhibited severe cracking upon preconditioning at 80°C (Fig. 3), which increased their permeability and caused the high VPV results recorded.

Baroghel-Bouny [50] proposed a classification of the durability of reinforced concrete structures based on "universal" durability indicators determined on a broad range of concretes cured in water. According to the proposed system, concrete mixes with VPV between 6-9% are categorised as highly durable. The VPV values of all the mixes examined in this study are lower than 6%, after 300 days of curing, even when rubber particles are used as partial aggregate replacement, which puts them in the highly durable category.

3.5.2 Oxygen permeability

The oxygen permeability is not only influenced by the overall porosity, but also by the proportion of continuity of larger pores where most of the flow will occur [51, 52]. Fig. 13 shows the oxygen permeability results for 28 day cured specimens (preconditioned at 80 ºC) and 300 day cured specimens (preconditioned at 40 ºC), expressed as the intrinsic permeability 'K'. Error bars correspond to one standard deviation of three measurements. Due to the extremely high permeability of the specimens resulting from the surface cracking upon preconditioning at 80°C, the gas permeability for the 28 day cured specimens with rubber particles could not be determined (the oxygen found its way out very quickly).

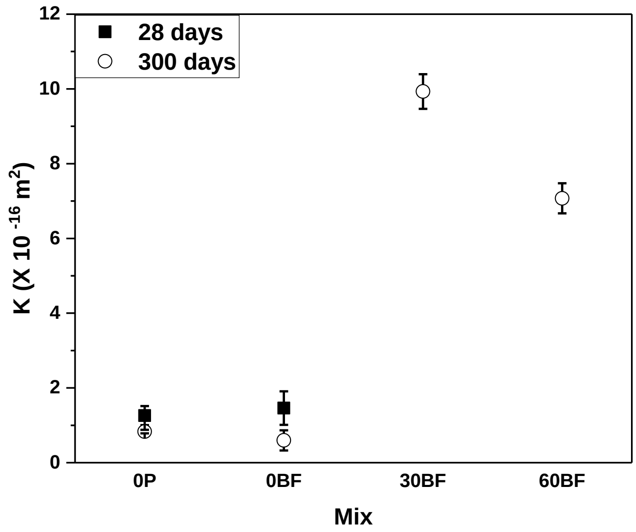

Fig. 13 Oxygen permeability results for all tested mixes

Considering the standard deviations as well as the experimental errors for both 28 and 300 days results, the oxygen permeability values for SFRC specimens, 0BF, are comparable with those of plain concrete, 0P, indicating that the fibres did not modify much the permeability of the concretes tested. SFRRuC specimens, 30BF and 60BF, on the other hand, show significantly higher permeability values, up to 12 and 8.5 times respectively, with respect to the plain concrete mix, 0P. These concretes presented comparable air contents (Table 4) and VPV values (Fig 12b), despite the differences in rubber content. The increased oxygen permeability recorded for the assessed specimens may be attributed to the compressibility of rubber particles when pressure is applied. If that is the case, then gas permeability may not be the best way to determine the permeability of RuC.

3.5.3 Water sorptivity

The main mechanism that governs sorptivity is capillary suction of water when a specimen is partially saturated [51, 53]. The difference in pressure causes the movement of water front through a porous material. Hence, sorptivity is derived by measuring the slope of the amount of water uptake per unit area as a function of the square root of time. The sorptivity results measured for 28 and 300 days cured specimens are shown in Fig. 14. Error bars correspond to one standard deviation of two measurements

For the 28 day cured samples, the addition of fibres to plain concrete, mix 0BF, causes marginal decrease in the sorptivity value, with an average of 12% with respect to the plain concrete mix, 0P. For 300 day, however, 0BF specimens record marginally higher sorptivity values, with an average of 9%, than that of 0P specimens. These results are in good agreement with the VPV values (Fig 12.b) confirming that the extended curing time had only a minor effect on the sorptivity and on the already high quality of the concrete matrix evaluated in this study.

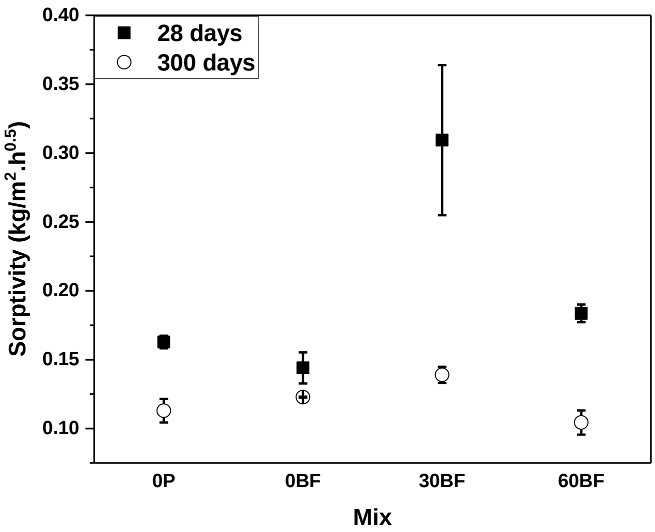

Fig. 14 Initial and secondary sorptivity values of all tested mixes

The 28 days sorptivity results of the SFRRuC specimens show different trends. While the 30BF specimens record the highest sorptiviy values, an average 90% higher than 0P mix, 60BF specimens shows slightly higher sorptivity value, average of 13% compared to 0P. In addition to the surface cracking upon preconditioning at 80°C, the high values of sorptivity for the 30BF specimens may be attributed to the large amount of fine pores which dominated the initial sorptivity behaviour, and hence increased the capillary suction. According to Assié et al. [54], the finer the pores the higher the capillary forces and thus the greater the tendency to imbibe water. On the other hand, the high amount of large course rubber particles in the 60BF specimens, especially those located in the concrete surface in contact with water (see Fig. 15), could have limited the water absorption rate (owing to the non-sorptive nature of rubber particles) and dominated the initial sorptivity behaviour.

Extending the curing time for 30BF and 60BF, i.e. 300 days, cause significant reduction in the sorptivity values, with average of 67% and 20%, respectively, when compared with the values registered for concretes cured for 28 days. This is mainly related to the absence of surface cracking upon preconditioning at 40°C which results in more realistic sorptivity values.

30BF **60BF**

Fig. 15 Cross section view of the SFRRuC specimens used for the sorptivity test

When calculating the concrete sorptivity using the depth penetration approach [51, 55, 56], all mixes examined here record sorptivity values less than 6 mm/h$^{0.5}$, which places them in the excellent durability class based on the durability index proposed by Alexander et al. [57] and adopted in [51, 55, 56].

3.6. Chloride ion penetration

Fig. 16 shows the chloride penetration zone after spraying 0.1 N $AgNO_3$ at the end of 90 and 150 days of chloride exposure in fully-saturated and wet-dry conditions. It is worth noting that it was not possible to detect the change in colour in any of the specimens exposed to chlorides for 300 days due to the dark colour of the concrete at this time, owing to the darkness of both the silica fume and rubber particles added. This drawback of the colorimetric method for assessing chloride permeability in concretes containing blended cement and silica fume has also been previously reported [58].

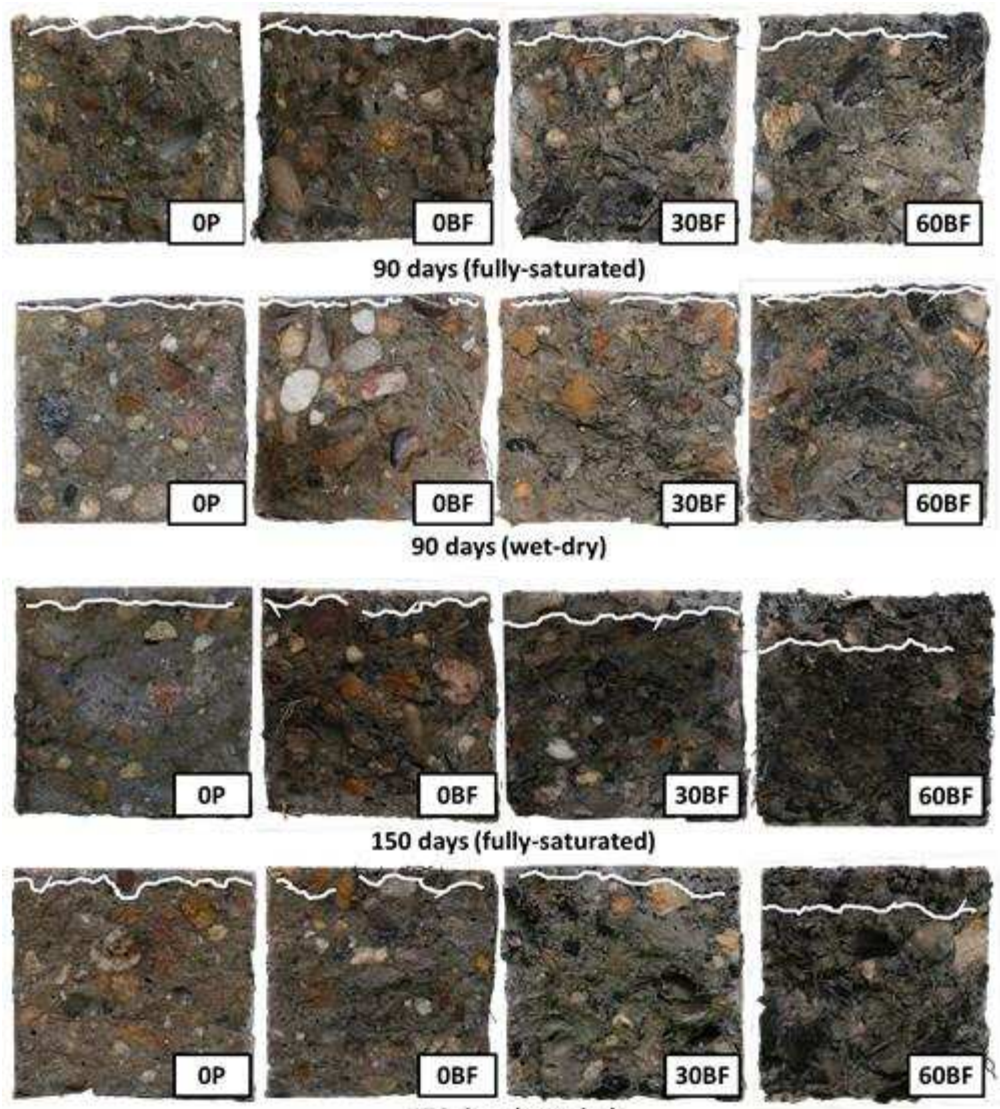

Fig. 16 Chloride contaminated zone of all concrete mixes at the end of 90 and 150 days of chloride exposure in fully-saturated and we-dry conditions

Fig. 17 shows a comparison between the average chloride penetration depths for all concrete specimens. Error bars correspond to one standard deviation of the average depth measured in two different specimens. For concretes exposed to wet-dry cycles, the chloride penetration depth is in general lower than those of fully-saturated specimens. In fully-saturated specimens the chloride ingress is mainly governed by the diffusion mechanism. The process of chloride ingress into concrete exposed to wet-dry cycles is a combination of diffusion and absorption, as in partially saturated concretes the chloride solution is absorbed by capillary suction and concentrated by evaporation of water [59]. These results somehow contradict what has been reported for other blended cement concretes [59], where the wet-dry cycle exposure to chlorides typically leads to deeper chloride penetration compared to fully-saturated ones. The duration of the wet-dry cycles, and particularly the degree of dryness achieved, controls the extent of ingress of chlorides, as higher degrees of dryness facilitate deeper chloride penetration during subsequent wet cycles [60]. Due to the low permeability of these concretes, it seems the drying cycle was not sufficient to remove water beyond the concrete surface, hindering capillary sorption of chlorides into the concrete.

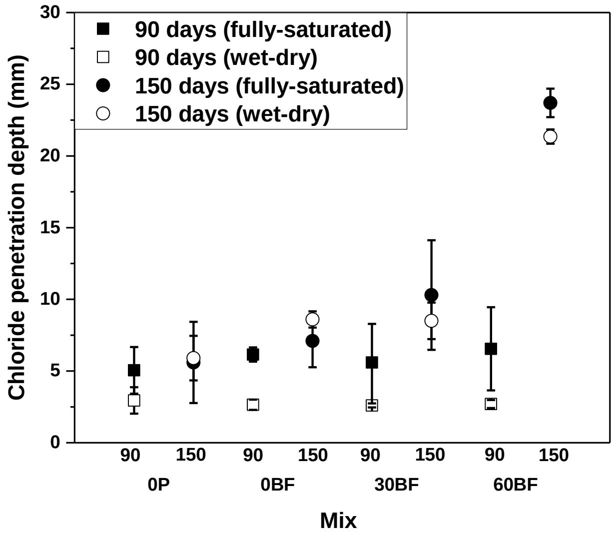

Fig. 17 Chloride penetration depth for all concrete mixes assessed at the end of 90 and 150 days of chloride exposure in fully-saturated and we-dry conditions

The data presented in Fig. 17 also indicate that the chloride penetration depth at the end of 90 days of exposure was small and comparable, being in the range of 5–7 mm for the fully-saturated specimens, and 2–3 mm for the wet-dry specimens. This suggests that up to 90 days of chloride exposure, the penetration rate was not aggravated by the addition of rubber. At the end of 150 days of chloride exposure, however, the depth of chloride penetration in both conditions generally increased with rubber content. This is consistent with the higher values of VPV obtained for SFRRuC specimens (sections 3.5.1).

For practical purposes, due to the small chloride penetration depths at 90 days and difficulty in identifying chloride penetration depths at 300 days of chloride exposure, only specimens at 150 days of exposure (in both conditions) were considered for the determination of total chloride concentration and apparent chloride diffusion coefficient. Table 5 presents the total chloride concentrations by weight of binder as well as the apparent chloride diffusion coefficient measured at the colour change boundary for all of the assessed concretes. The chloride concentrations for the plain concrete and SFRC mixes, 0P and 0BF, were less than 10 ppm, hence it was not possible to detect the exact total chloride concentrations and then calculate the apparent diffusion coefficients for these mixes.

Table 5. Chloride concentration and apparent chloride diffusion coefficient in concretes after 150 days of chlorides exposure

Mix	Chloride concentration %wt of binder		Apparent diffusion coefficient (10^{-12} m^2/s)	
	fully-saturated	wet-dry	fully-saturated	wet-dry
0P	<10 ppm	<10 ppm	-	-
0BF	<10 ppm	<10 ppm	-	-
30BF	0.109	0.234	1.89	1.83
60BF	0.151	0.157	7.74	3.92

SFRRuC mixes, 30BF and 60BF, present lower chloride concentrations values (at both conditions) than 0.4% by weight of cement, which is the most commonly assumed critical total chloride concentration value inducing corrosion [58, 61]. This indicates that even with the increased VPV and sorptivity caused by the replacement of natural aggregates with rubber particles (Section 3.5.1 and 3.5.3), the assessed concretes present high resistance to chloride permeability.

SFRRuC mixes, 30BF and 60BF, show an increase in the apparent chloride diffusion coefficient at higher rubber contents, possibly due to their higher VPV and sorptivity. The apparent chloride diffusion coefficients of the fully-saturated and wet-dry specimens are comparable for the 30BF mixes, indicating that under the testing conditions used in this study, the drying cycle had a negligible effect on chloride permeability. Similar results have been identified in high quality Portland cement based concretes produced with silica fume, due to their refined porosity requiring longer drying times to obtain a particular moisture content [59]. On the other hand, 60BF specimen in fully-saturated condition registers twice the diffusion coefficient than that in wet-dry condition. Nevertheless, with the apparent diffusion coefficients values observed here, SFRRuC mixes can be consider as highly durable concrete mixes according to the durability indicators suggested by Assié et al. [54].

For inspection purposes, the authors collected concrete samples at 50 mm depth from the exposed surface from those specimens exposed to chloride for 300 days, in both conditions, and the total chloride concentrations were measured. The total chloride concentrations for all of the examined samples were less than 10 ppm. This confirms the good resistance to chloride penetrability of all mixes.

4 Conclusion

This study examined the fresh, mechanical and permeability properties as well as chloride corrosion effects due to an exposure to accelerated marine environment of SFRRuC. Natural aggregates were partially replaced with waste tyre rubber particles and blends of manufactured steel fibres and recycled tyre steel fibres were used as reinforcement. Based on the experimental results, the following conclusions can be drawn:

- The addition of fibres marginally decreases workability and increases air content and unit weight. The substitution of rubber aggregates in SFRRuC mixes significantly reduces workability and unit weight (due to the lower density of rubber) and increases air content by more than 100%.

- No visual signs of deterioration or cracks (except superficial rust) were observed on the surface of concrete specimens subjected to 150 or 300 days of accelerated chloride exposure. Furthermore, no evidence of rust is observed internally on the fibres embedded in concretes indicating that steel reinforcement did not corrode to any significant extent under the wet-dry chloride exposure.

- The use of increasingly higher volumes of rubber aggregate in SFRRuC mixes reduces progressively the compressive strength and elastic modulus of concrete. Flexural strength is also affected, though to a lesser extent due to the presence of fibres. Hence, fibres are a key component when RuC is to be used for structural pavement purposes.

- As a consequence of the ongoing hydration of the cementitious materials, a slight general increase in the mechanical properties of all mixes after 150 and 300 days of wet-dry chloride exposure was identified in comparison to the 28-day mechanical properties.

- While VPV and sorptivity generally increase with increased rubber content, the change with respect to plain concrete is minor. All mixes examined after 300 days of mist curing show VPV values lower than 6% and sorptivity values lower than 6 mm/h$^{0.5}$, which means that they can be classified as highly durable concrete mixes.

- Due to the compressibility of rubber particles when pressure is applied, the oxygen permeability test can produce misleading results when evaluating RuC mixes with high amounts of rubber.

- The depth of chloride penetration in both conditions (fully-saturated and wet-dry) generally increases with rubber content. At the colour change boundary, 30BF and 60BF specimens record lower chloride concentrations than 0.4% by weight of cement (critical concentration inducing corrosion) and present apparent diffusion coefficients values within the range of highly durable concrete mixes.

It is concluded that SFRRuC is a promising candidate material for use in structural concrete applications with increased toughness and flexibility requirements as well as good transport and permeability characteristics. Future work should be directed towards investigating the long-term performance of this innovative concrete in aggressive environments such as freeze-thaw resistance and fatigue performance.

Acknowledgements

The research leading to these results has received funding from the European Union Seventh Framework Programme [FP7/2007- 2013] under grant agreement n° 603722. The authors would also like to thank all of the material suppliers and companies for their in-kind contribution for this research study: Tarmac UK, Sika, Aggregate Industries UK Ltd and Twincon Ltd. The first author PhD studies are sponsored by King Saud University and the Ministry of Education in the Kingdom of Saudi Arabia.

References

1. Alsaif, A., et al., *Mechanical performance of steel fibre reinforced rubberised concrete for flexible concrete pavements.* Construction and Building Materials, 2018. **172**: p. 533-543.
2. Raffoul, S., et al., *Behaviour of unconfined and FRP-confined rubberised concrete in axial compression.* Construction and Building Materials, 2017. **147**: p. 388-397.
3. Hernández-Olivares, F. and G. Barluenga, *Fire performance of recycled rubber-filled high-strength concrete.* Cement and Concrete Research, 2004. **34**(1): p. 109-117.
4. Eldin, N.N. and A.B. Senouci, *Measurement and prediction of the strength of rubberized concrete.* Cement and Concrete Composites, 1994. **16**(4): p. 287-298.
5. Medina, N.F., et al., *Mechanical and thermal properties of concrete incorporating rubber and fibres from tyre recycling.* Construction and Building Materials, 2017. **144**: p. 563-573.
6. Flores-Medina, D., N.F. Medina, and F. Hernández-Olivares, *Static mechanical properties of waste rests of recycled rubber and high quality recycled rubber from crumbed tyres used as aggregate in dry consistency concretes.* Materials and Structures, 2014. **47**(7): p. 1185-1193.
7. Benazzouk, A., et al., *Physico-mechanical properties and water absorption of cement composite containing shredded rubber wastes.* Cement and Concrete Composites, 2007. **29**(10): p. 732-740.
8. Liu, F., et al., *Mechanical and fatigue performance of rubber concrete.* Construction and Building Materials, 2013. **47**: p. 711-719.
9. Raffoul, S., et al., *Optimisation of rubberised concrete with high rubber content: An experimental investigation.* Construction and Building Materials, 2016. **124**: p. 391-404.
10. Grinys, A., et al., *Fracture of concrete containing crumb rubber.* Journal of Civil Engineering and Management, 2013. **19**(3): p. 447-455.
11. Khatib, Z. and F. Bayomy, *Rubberized portland cement concrete.* Journal of Materials in Civil Engineering, 1999. **11**(3): p. 206-213.
12. Khaloo, A.R., M. Dehestani, and P. Rahmatabadi, *Mechanical properties of concrete containing a high volume of tire–rubber particles.* Waste Management, 2008. **28**(12): p. 2472-2482.
13. Xie, J.-H., et al., *Compressive and flexural behaviours of a new steel-fibre-reinforced recycled aggregate concrete with crumb rubber.* Construction and Building Materials, 2015. **79**: p. 263-272.
14. Turatsinze, A. and M. Garros, *On the modulus of elasticity and strain capacity of self-compacting concrete incorporating rubber aggregates.* Resources, conservation and recycling, 2008. **52**(10): p. 1209-1215.
15. Onuaguluchi, O. and D.K. Panesar, *Hardened properties of concrete mixtures containing pre-coated crumb rubber and silica fume.* Journal Of Cleaner Production, 2014. **82**: p. 125-131.
16. Bravo, M. and J. de Brito, *Concrete made with used tyre aggregate: durability-related performance.* Journal of Cleaner Production, 2012. **25**: p. 42-50.
17. Benazzouk, A., O. Douzane, and M. Quéneudec, *Transport of fluids in cement–rubber composites.* Cement and Concrete Composites, 2004. **26**(1): p. 21-29.
18. Segre, N. and I. Joekes, *Use of tire rubber particles as addition to cement paste.* Cement And Concrete Research, 2000. **30**(9): p. 1421-1425.
19. Gesoğlu, M. and E. Güneyisi, *Permeability properties of self-compacting rubberized concretes.* Construction and Building Materials, 2011. **25**(8): p. 3319-3326.
20. Gesoglu, M. and E. Guneyisi, *Strength development and chloride penetration in rubberized concretes with and without silica fume.* Materials and Structures, 2007. **40**(9): p. 953-964.
21. Kardos, A.J. and S.A. Durham, *Strength, durability, and environmental properties of concrete utilizing recycled tire particles for pavement applications.* Construction and Building Materials, 2015. **98**: p. 832-845.
22. Topçu, İ.B. and A. Demir, *Durability of rubberized mortar and concrete.* Journal Of Materials In Civil Engineering, 2007. **19**(2): p. 173-178.

23. Marcos-Meson, V., et al., *Corrosion resistance of steel fibre reinforced concrete - A literature review.* Cement and Concrete Research, 2018. **103**: p. 1-20.
24. BSI, *EN 197-1: Cement — Part 1: Composition, specifications and conformity criteria for common cements. BSI 389 Chiswick High Road, London W4 4AL, UK.* 2011.
25. ASTM, *C136: Standard test method for sieve analysis of fine and coarse aggregates. ASTM International, West Conshohocken, PA. doi:10.1520/C0136-06.* 2006.
26. BSI, *EN 12390-2: Testing hardened concrete, Part 2: Making and curing specimens for strength tests. BSI 389 Chiswick High Road, London W4 4AL, UK.* 2009.
27. BSI, *EN 12350-2: Testing fresh concrete, Part 2: Slump-test. BSI 389 Chiswick High Road, London W4 4AL, UK.* 2009.
28. BSI, *EN 12350-7: Testing fresh concrete, Part 7: Air content — Pressure. BSI 389 Chiswick High Road, London, W4 4AL, UK.* 2009.
29. BSI, *EN 12350-6: Testing fresh concrete Part 6: Density. BSI 389 Chiswick High Road, London, W4 4AL, UK.* 2009.
30. BSI, *EN 12390-3: Testing hardened concrete, Part3: Compressive strength of test specimens. BSI 389 Chiswick High Road, London W4 4AL, UK.* 2009.
31. RILEM, *TC 162-TDF: Test and design methods for steel fibre reinforced concrete, Bending test, Final Reccomendation. Materials and Structures: 35, 579-582.* 2002.
32. JSCE, *SF-4: Method of test for flexural strength and flexural toughness of steel fiber reinforced concrete. Japan Concrete Institute, Tokio, Japan.* 1984.
33. Feldman, R.F. and V.S. Ramachandran, *Differentiation of interlayer and adsorbed water in hydrated Portland cement by thermal analysis.* Cement And Concrete Research, 1971. **1**(6): p. 607-620.
34. Farage, M., J. Sercombe, and C. Galle, *Rehydration and microstructure of cement paste after heating at temperatures up to 300 C.* Cement And Concrete Research, 2003. **33**(7): p. 1047-1056.
35. Graeff, A., *Long Term Performance of Recycled Steel Fibre Reinforced Concrete for Pavement Applications*, in *Department of Civil and Structural Engineering*. 2011, The University of Sheffield: Sheffield.
36. BSI, *EN 13057:2002: Products and systems for the protection and repair of concrete structures - Test methods - Determination of resistance of capillary absorption. BSI 389 Chiswick High Road, London W4 4AL, UK.* 2002.
37. ASTM, C., *1202.* Rapid Chloride Permeability, 1997.
38. BSI, *EN 12390-11: Testing hardened concrete - Part 11: Determination of the chloride resistance of concrete, unidirectional diffusion. BSI 389 Chiswick High Road, London W4 4AL, UK.* 2015.
39. NordTest, *NT Build 492, Chloride migration coefficient from non-steady state migration experiments*. 1999.
40. Ismail, I., et al., *Influence of fly ash on the water and chloride permeability of alkali-activated slag mortars and concretes.* Construction and Building Materials, 2013. **48**: p. 1187-1201.
41. Siddique, R. and T.R. Naik, *Properties of concrete containing scrap-tire rubber–an overview.* Waste Management, 2004. **24**(6): p. 563-569.
42. Mangat, P. and B. Molloy, *Size effect of reinforcement on corrosion initiation. in: P. Rossi, G. Chanvillard (Eds.), PRO 15 5th RILEM Symp. Fibre-reinforced Concrete. BEFIB, RILEM Publications SARL, Lyon, France, 2000. pp. 691–701.*
43. Mangat, P. and K. Gurusamy, *Chloride diffusion in steel fibre reinforced marine concrete.* Cement And Concrete Research, 1987. **17**(3): p. 385-396.
44. Mangat, P.S. and K. Gurusamy, *Chloride diffusion in steel fibre reinforced concrete containing PFA.* Cement and Concrete Research, 1987. **17**(4): p. 640-650.
45. Hu, H., et al., *Mechanical properties of SFRC using blended manufactured and recycled tyre steel fibres.* Construction and Building Materials, 2018. **163**: p. 376-389.

46. Frazão, C., et al., *Corrosion effects on pullout behavior of hooked steel fibers in self-compacting concrete.* Cement and Concrete Research, 2016. **79**: p. 112-122.
47. Singh, A.P. and D. Singhal, *Permeability of steel fibre reinforced concrete influence of fibre parameters.* Procedia Engineering, 2011. **14**: p. 2823-2829.
48. Karahan, O., et al., *Fresh, Mechanical, Transport, and Durability Properties of Self-Consolidating Rubberized Concrete.* Aci Materials Journal, 2012. **109**(4).
49. Sukontasukkul, P. and K. Tiamlom, *Expansion under water and drying shrinkage of rubberized concrete mixed with crumb rubber with different size.* Construction And Building Materials, 2012. **29**: p. 520-526.
50. Baroghel-Bouny, V. *Evaluation and prediction of reinforced concrete durability by means of durability indicators. Part I: new performance-based approach*. in *ConcreteLife'06-International RILEM-JCI Seminar on Concrete Durability and Service Life Planning: Curing, Crack Control, Performance in Harsh Environments*. 2006: RILEM Publications SARL.
51. Du Preez, A. and M. Alexander, *A site study of durability indexes for concrete in marine conditions.* Materials and structures, 2004. **37**(3): p. 146-154.
52. Mackechnie, J.R., *Predictions of reinforced concrete durability in the marine environment*. 1995, University of Cape Town.
53. Pelisser, F., et al., *Concrete made with recycled tire rubber: effect of alkaline activation and silica fume addition.* Journal Of Cleaner Production, 2011. **19**(6): p. 757-763.
54. Assié, S., G. Escadeillas, and V. Waller, *Estimates of self-compacting concrete 'potential'durability.* Construction and Building Materials, 2007. **21**(10): p. 1909-1917.
55. Olorunsogo, F. and N. Padayachee, *Performance of recycled aggregate concrete monitored by durability indexes.* Cement And Concrete Research, 2002. **32**(2): p. 179-185.
56. Alexander, M. and B. Magee, *Durability performance of concrete containing condensed silica fume.* Cement And Concrete Research, 1999. **29**(6): p. 917-922.
57. Alexander, M., J. Mackechnie, and Y. Ballim, *Guide to the use of durability indexes for achieving durability in concrete structures.* Research monograph, 1999. **2**.
58. Baroghel-Bouny, V., et al., *$AgNO_3$ spray tests: advantages, weaknesses, and various applications to quantify chloride ingress into concrete. Part 1: Non-steady-state diffusion tests and exposure to natural conditions.* Materials and Structures, 2007. **40**(8): p. 759-781.
59. Hong, K. and R.D. Hooton, *Effects of cyclic chloride exposure on penetration of concrete cover.* Cement and Concrete Research, 1999. **29**(9): p. 1379-1386.
60. Neville, A.M., *Properties of Concrete, 4th Ed.* 1996, Harlow, UK: John Wiley & Sons. 844.
61. Glass, G. and N. Buenfeld, *The presentation of the chloride threshold level for corrosion of steel in concrete.* Corrosion science, 1997. **39**(5): p. 1001-1013.